Proc. R. Soc. London Ser. B **264**, 297 (1997).
4. M. Petrie, *Nature* **371**, 598 (1994).
5. M. Kirkpatrick and N. H. Barton *Proc. Natl. Acad. Sci. U.S.A.* **94**, 1282 (1997).
6. G. M. Klump and H. C. Gerhardt, *Nature* **326**, 286 (1987).
7. H. C. Gerhardt, M. L. Dyson, S. D. Tanner, *Behav. Ecol.* **7**, 7 (1996).
8. B. K. Sullivan and S. H. Hinshaw, *Anim. Behav.* **44**, 733 (1992).
9. G. M. Fellers, *Copeia* **1979**, 286 (1979).
10. J. D. Krenz, unpublished data.
11. K. D. Wells and T. L. Taigen, *Behav. Ecol. Sociobiol.* **19**, 9 (1986).
12. H. C. Gerhardt, *Anim. Behav.* **42**, 615 (1991).
13. L. S. Runkle, K. D. Wells, C. C. Robb, S. L. Lance, *Behav. Ecol.* **5**, 318 (1994).
14. U. Grafe, *Copeia* **1997**, 356 (1997).
15. H. C. Gerhardt and G. F. Watson, *Anim. Behav.* **50**, 1187 (1995); H. C. Gerhardt and S. D. Tanner, unpublished data.
16. In 1995, average numbers of pulses per call ranged from 15.3 to 21.8 for individual short-callers and from 22.1 to 38.7 for long-callers. In 1996, average pulse numbers ranged from 14.4 to 18.0 for short-callers and from 22.1 to 37.7 for long-callers.
17. R. D. Semlitsch, S. Schmiedehausen, H. Hotz, P. Beerli, *Evol. Ecol.* **10**, 531 (1996); R. D. Semlitsch, H. Hotz, G.-D. Guex, *Evolution* **51**, 1249 (1997).
18. D. S. Falconer and T. F. C. Mackay, *Introduction to Quantitative Genetics* (Longman, Essex, ed. 4, 1996).
19. Tadpoles were fed finely ground Tetra-Min fish flakes. The high food ration was typically as much as the tadpoles could consume and was always three times the low food ration. Larval survival, growth rate, length of larval period, and mass at metamorphosis differed significantly between the two food levels in both years ($P < 0.001$, t tests), demonstrating that the low food level constituted a significantly less favorable environment than the high food level.
20. Individuals metamorphosing from our high food treatment weighed an average of 0.359 g in 1995 and 0.319 g in 1996. Average mass at metamorphosis of *H. versicolor* reared in field enclosures was 0.340 g in the sun and 0.310 g in the shade (*13*). In a natural population of *H. chrysoscelis* (the cryptic sister species of *H. versicolor*), average mass at metamorphosis was 0.33 g (*28*).
21. Tadpoles were randomly assigned to food levels and blocks within our randomized block design. The experiment was conducted blind with respect to genetic identity.
22. Performance was measured as follows: wet mass (to the nearest milligram) on day 30 of the experiment—a measure of early larval growth rate; the larval period in days from the beginning of the experiment (stage 25) (*29*) to forelimb emergence (stage 42); and wet mass (to the nearest milligram) of metamorphs after tail resorption (stage 46). Larval survival was calculated as the proportion of individuals from each family surviving to metamorphosis. In 1996, postmetamorphic growth was calculated as the difference between wet mass achieved 30 days after metamorphosis and wet mass at metamorphosis.
23. K. A. Berven and D. E. Gill, *Am. Zool.* **23**, 85 (1983); D. C. Smith, *Ecology* **68**, 344 (1987).
24. Mixed-model univariate analyses of variance (ANOVAs) were performed for each response variable, at each food level during each year, to test for the main effects of call duration, maternal identity, paternal identity (1996 only), and blocking factors, as well as for interactions. In order to account for correlations between larval period and metamorphic mass, each was used as a covariate in the univariate analyses of the other. Metamorphic mass was also used as a covariate in analyses of postmetamorphic growth. ANOVA tables and more complete descriptions of analyses can be found at www.sciencemag.org/feature/data/976682.shl
25. A multivariate analysis of variance (MANOVA) was used for each food level during each year to test for multivariate effects of call duration, maternal identity, paternal identity (1996 only), and blocking factors. MANOVAs simultaneously included larval growth, larval period, metamorphic mass, and (in 1996) postmetamorphic growth but did not include survival because the unit of analysis for this variable was the family rather than the individual. We present results for the multivariate effect of call duration, based on Wilks' λ. Data were appropriately transformed in both univariate and multivariate analyses.
26. R. R. Sokal and F. J. Rohlf, *Biometry* (Freeman, San Francisco, 1981).
27. H. M. Wilbur and J. P. Collins, *Science* **182**, 1305 (1973); J. Travis, *Evolution* **44**, 502 (1984).
28. M. E. Ritke, J. G. Babb, M. K. Ritke, *J. Herpetol.* **24**, 135 (1990).
29. K. L. Gosner, *Herpetologica* **16**, 183 (1960).
30. We thank B. Buchanan and J. Schwartz for help in assessing males in 1996; J. Krenz for help with artificial crosses in 1996; A. Bullerdieck for assistance in raising tadpoles in 1996; M. Cherry, M. Cunningham, J. Krenz, M. Parris, A. Pomiankowski, T. Ryan, and J. Schwartz for comments on the manuscript; and the many people who helped collect frogs. This work was supported by an NSF predoctoral fellowship (A.M.W.), NSF and NIMH grants (H.C.G.), and a Sigma Xi Grant-in-aid of Research (A.M.W.).

12 December 1997; accepted 22 April 1998

Neural Correlates of Perceptual Rivalry in the Human Brain

Erik D. Lumer,* Karl J. Friston, Geraint Rees

When dissimilar images are presented to the two eyes, perception alternates spontaneously between each monocular view, a phenomenon called binocular rivalry. Functional brain imaging in humans was used to study the neural basis of these subjective perceptual changes. Cortical regions whose activity reflected perceptual transitions included extrastriate areas of the ventral visual pathway, and parietal and frontal regions that have been implicated in spatial attention; whereas the extrastriate areas were also engaged by nonrivalrous perceptual changes, activity in the frontoparietal cortex was specifically associated with perceptual alternation only during rivalry. These results suggest that frontoparietal areas play a central role in conscious perception, biasing the content of visual awareness toward abstract internal representations of visual scenes, rather than simply toward space.

Binocular rivalry provides a useful experimental paradigm with which to study the neural correlates of conscious perception (*1*–*3*). When dissimilar images are presented to the two eyes, they compete for perceptual dominance so that each image is visible in turn for a few seconds while the other is suppressed. Because perceptual transitions between each monocular view occur spontaneously without any change in the physical stimulus, neural responses associated with perceptual processes can be distinguished from those due to stimulus characteristics. Recent neurophysiological studies in awake monkeys have established that, whereas the firing of most neurons in primary visual cortex (V1) correlates with the stimulus and not the percept during rivalry, activity of neurons at higher levels in the visual pathway, such as in the inferotemporal cortex, reflects the perceptual state (*3*). These findings suggest that rivalry results from a competition between alternative stimulus interpretations at a level beyond the stages of monocular processing early in visual cortex (*4*). Psychophysical observations also suggest that perceptual alternation during rivalry results from the same neural operations underlying other multistable perceptual phenomena, such as depth reversals and ambiguous figures, that show similar temporal dynamics to binocular rivalry (*5*). Although less pronounced, similar perceptual fluctuations can also be experienced in normal vision and may therefore reflect a basic perceptual strategy to resolve visual ambiguity (*6*). Yet despite significant interest in the neural correlates of binocular rivalry (*1*–*3*), the mechanisms underlying these perceptual alternations remain unknown.

Here we investigate these mechanisms by characterizing neural activity associated with perceptual transitions per se, rather than activity associated with perceptual state during rivalry. Our results provide evidence for an involvement not only of occipitotemporal visual areas in binocular rivalry, but also indicate a specific and previously unknown role for frontoparietal areas in mediating the perceptual transitions experienced during rivalry. These results were obtained by measuring brain activity with functional magnetic resonance imaging (fMRI) in humans who reported their percepts under two different viewing conditions (*7*). In the first condition, subjects viewed dichoptic stimuli consisting of a red-colored drifting grating shown to one eye and a green-colored face shown to the other eye. These images were chosen because they are highly dissimilar and readily produce full-field rivalry when

Wellcome Department of Cognitive Neurology, Institute of Neurology, University College London, Queen Square, London WC1N 3BG, UK.

*To whom correspondence should be addressed. E-mail: elumer@fil.ion.ucl.ac.uk

viewed through stereoscopic glasses. By manipulating the contrast setting in each image, we were able to bias perceptual dominance in favor of the grating, with long periods during which the grating was seen alone interrupted by shorter incursions of the face in conscious perception (Fig. 1) (*8*). Subjects used key presses to signal perceptual alternations from the grating to the face or vice versa. To control for motor effects, we compared the activity evoked during rivalry to that elicited in a second, nonrivalrous viewing condition that required the same type of motor responses. In this second condition, subjects were exposed to a "replay" of their perception during rivalry. This was achieved by presenting, in a chronology specified by the key reports during rivalry, either the face alone or the grating alone to one eye, and a gray patch of comparable luminance to the other eye. At transition times, physical blends of the face and grating were shown. This stimulation was designed to produce a perception that closely mimics rivalry in both quality and timing, thus resulting in a matched sequence of motor reports in the two conditions (*9*). Because prolonged periods of stereoscopic fusion can cause ocular fatigue, a third, passive condition was also introduced during scanning to allow visual rest.

Functional MRI scans from six participants were analyzed as a group to identify brain areas where activity was consistently correlated with the perceptual changes reported during either viewing condition (*10*, *11*). To distinguish transient activity associated specifically with perceptual alternation from other, nonselective effects of viewing condition, we modeled the predicted hemodynamic response to each transition event and tested for the presence of such responses in the data while treating the mean condition-specific effects as confounds. Such an event-related modulation of the fMRI signals reflects neural activity that is locked to the time of occurrence of perceptual transitions between face and grating. During rivalry, transient responses associated with shifts of perception were found bilaterally in extrastriate areas of the fusiform gyrus, in right inferior and superior parietal lobules, and in bilateral inferior frontal, middle frontal, and insular cortex (Fig. 2 and Table 1). Event-related activity was also observed in regions of the anterior cingulate cortex, supplementary motor area (SMA), and left primary motor and somatosensory cortex, consistent with the preparation and execution of appropriate motor reports. The estimated hemodynamic response to single transition events is shown for a representative region of activation in Fig. 2 as a function of postevent time (*12*).

Although neural correlates of rivalrous transitions were expressed at multiple levels of the visual occipitotemporal pathway, such correlates were not observed in primary visual cortex. Perceptual transitions experienced during dichoptic stimulation were highly correlated with activity in extrastriate areas concerned with the representation of higher order properties of the visual scene (*13*). In particular, we detected transient responses that reflected these perceptual changes in regions of the fusiform gyri that included areas previously implicated in the perception of faces (*14*). By contrast to higher visual areas, early visual cortical areas showed no significant modulation of activity during rivalrous transitions. The differential involvement of early and higher visual cortical areas in rivalry was further confirmed by an analysis of activity correlated with the perceptual state rather than with the perceptual transitions reported by the subjects (*15*). These results in humans are consistent with recent findings in monkeys, suggesting that rivalry reflects central processes that take effect subsequent to the analysis of both monocular stimuli (*3*, *4*).

By comparing rivalry to a nonrivalrous viewing condition, the present study also allowed us to provide an answer to the central issue in multistable perception—whether a specific machinery mediates the ongoing selection among sets of neuronal events competing for visual awareness. Because the rivalry and replay conditions yield similar perception and behavior, we expected them to engage common neural pathways associated with the internal representation of visual

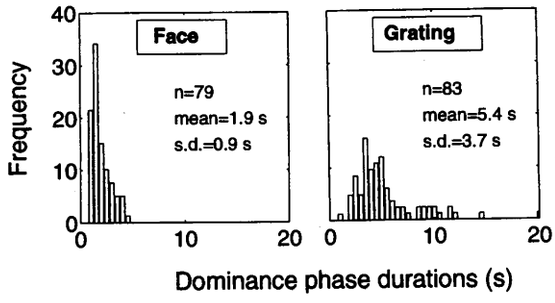

Fig. 1. Temporal dynamics of binocular rivalry during fMRI. The frequency histograms show the distribution of dominance times for face (left) and grating (right) reported by a representative subject while undergoing functional imaging. Mean dominance times averaged across subjects are given in (*8*).

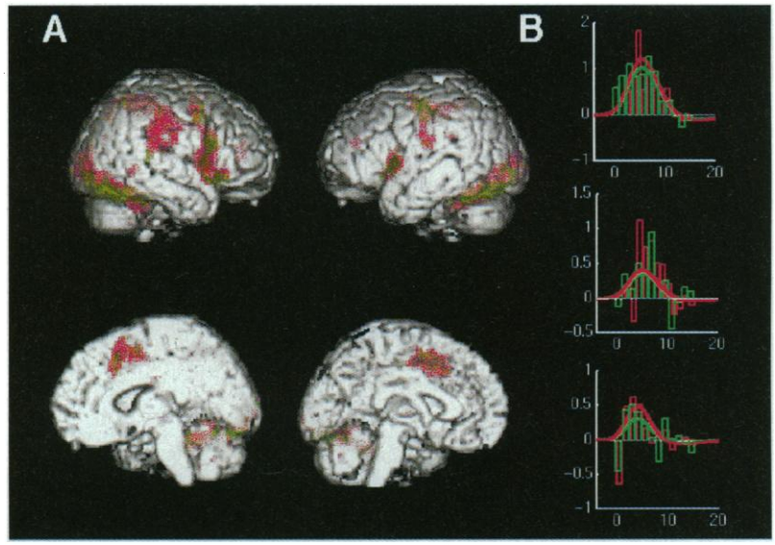

Fig. 2. Event-related activity during rivalry and replay conditions. (**A**) Four views of the medial and lateral surfaces of a rendering of the T1-weighted anatomical template image in Talairach space, on which are superimposed areas where evoked activity was specifically related to perceptual transitions in either the rivalry condition (red) or the replay condition (green). A statistical threshold of $Z = 3.09$ (corresponding to $P < 0.001$, uncorrected) was used for display purposes; peaks of activation reaching statistical significance after correction for multiple comparisons ($P < 0.05$) are listed in Table 1. The areas modulated by perception during both rivalrous and replay viewing, and the bilateral symmetry of the evoked activity are apparent. (**B**) Illustrative postevent histograms of the modulation of activity produced by transition events in rivalry (red) and replay (green) conditions from three different subjects. The evoked activity (percent change in BOLD contrast) is shown as a function of postevent time (in seconds) for each subject, with the fitted models of hemodynamic response function superimposed in solid lines. The modulation of activity shown here is taken from a voxel in right anterior fusiform gyrus ($x = 33$ mm, $y = -45$ mm, $z = -21$ mm; $Z = 8.10$, $P < 0.001$ corrected).

scenes and the generation of appropriate motor responses. This was confirmed by the fMRI data: Event-related activity during replay was similar to that evoked during rivalry in visual areas of the fusiform gyri and in areas associated with movement (Fig. 2 and Table 1) (*16*). However, the rivalry and replay conditions differ fundamentally in the way that they achieve alternating perception. Whereas perceptual shifts during rivalry derive from an endogenous neural instability in the absence of changes in the stimulus, during replay they rely on exogenous manipulation of the visual input. Hence, we reasoned that any differential event-related activity between the two conditions would reflect these differences. Such a contrast would expose the mechanisms underlying the ongoing selection between conflicting perceptual interpretations during rivalry, a conflict that is not evoked by the replay condition. In addition, we predicted that the early visual cortex may show less transient activity during rivalry than during replay, because dichoptic stimulation causes little modulation of neuronal activity and possible inhibition at this stage of processing (*3*, *17*), whereas repeated stimulus onset and offset as generated during replay typically evoke strong cortical responses.

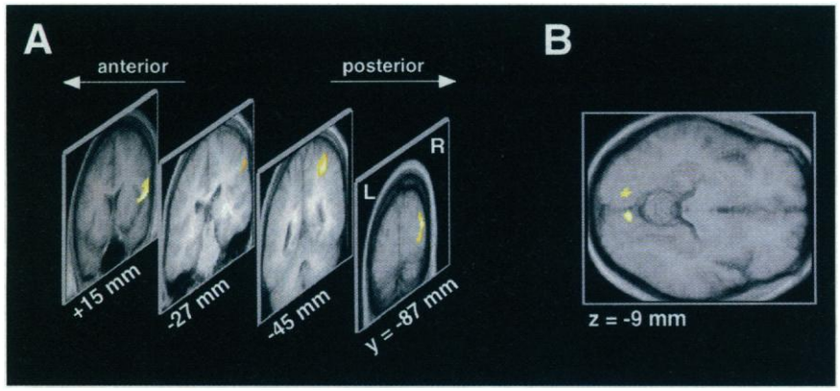

Fig. 3. Differential activation during rivalrous and nonrivalrous viewing. (**A**) Areas where transient activity related to perceptual shifts is greater under conditions of binocular rivalry compared with the replay condition, overlaid onto the average Talairach normalized anatomical MR image of the six subjects. Significant differential activation during rivalry ($P < 0.05$, corrected) is confined to the right hemisphere and involves frontoparietal structures previously implicated in the shifting of spatial attention. Distance from the anterior commissure is indicated for each coronal section. L, left; R, right. (**B**) A transverse section through the average normalized anatomical MR image, taken 9 mm below the bicommissural plane, on which are superimposed two foci of activation that represent early visual areas where activity related specifically in time to perceptual transitions is greater under conditions of replay compared with rivalry.

Table 1. Coordinates and *Z* scores for event-related activation. Shown in the table are loci where event-related activity is greater during replay compared with rivalry (replay > rivalry); modulation of activity above baseline is measured when viewing dichoptic stimuli (rivalry) or replayed scenes (replay); and event-related activity is greater during rivalry compared with replay (rivalry > replay). Only the most significant peaks within each area of activation are reported in the table ($P < 0.05$, corrected).

Cortical region	Talairach coordinates (mm)			*Z* score
	x	*y*	*z*	
	Rivalry			
Right fusiform	33	−45	−21	8.1
Left fusiform	−30	−69	−18	7.77
Medial anterior cingulate/SMA	0	0	48	7.21
	9	21	36	6.13
Right insula/frontal operculum	60	15	−3	8.11
Right inferior frontral	54	15	27	7.64
Left insula/frontal operculum	−57	9	3	7.33
Right superior parietal lobule	30	−54	54	7.53
Right inferior parietal lobule	60	−27	30	7.14
Left motor/somatosensory	−36	−12	57	7.33
Right middle frontal	39	42	18	5.49
Left middle frontal	−36	39	21	5.54
	Replay			
Right fusiform	33	−45	−21	7.44
Left fusiform	−27	−69	−18	7.48
Right insula/frontal operculum	57	21	−9	6.9
Right inferior frontral	54	15	24	6.35
Left insula/frontral operculum	−60	12	3	5.38
Right superior temporal	69	−36	9	5.42
Left motor/somatosensory	−39	−15	51	6.68
	Rivalry > replay			
Right inferior parietal	66	−30	36	5.79
Right superior parietal	36	−45	51	5.44
Right lateral extrastriate (BA 19)	42	−87	9	5.21
Right inferior frontal	51	15	−6	4.66
	Replay > rivalry			
Right BA 18	9	−75	−3	5.13
Left BA 18	−15	−78	−12	4.85

In contrast to the bilateral pattern of event-related activity in common across conditions, activity specific to the rivalry condition was strongly lateralized to the right hemisphere. Selective activation during rivalrous perceptual transitions was seen in a region of right extrastriate visual cortex, Brodmann area (BA) 19, and in the right inferior parietal, superior parietal, and inferior frontal cortex (Fig. 3 and Table 1). This pattern of activation was both highly significant and consistent across subjects. We also characterized areas where transient activity associated with perceptual alternations was greater during replay compared with rivalry. Areas that showed such differential activation were located in early visual cortex (medial portion of BA 18), in accord with our prior hypothesis (Fig. 3 and Table 1). The comparison between the rivalry and replay conditions demonstrates a double dissociation; right frontoparietal regions show greater transition-related activity during rivalry, whereas early visual cortex shows greater transient responses during nonrivalrous viewing. These differences cannot be attributed to the generation of motor reports because the two conditions entailed the same sequence of motor responses and produced similar activity in cortical areas associated with movement (*9*). It is also unlikely that this differential pattern of activity results from nonspecific differences in attentional demands between the two conditions, such as arousal or difficulty. Frontoparietal activity has not been observed during the performance of other visual tasks in which attentional demands were varied systematically (*18*). Moreover, changes in attentional demands typically result in different levels of activation in ventral areas involved in representation of visual scenes (*19*); such differences were not observed in the present study when the two viewing conditions were compared. Instead,

the present results are more consistent with the notion that a distributed frontoparietal system specifically mediates the perceptual switches experienced during rivalry.

Right frontoparietal areas have been traditionally implicated in visual tasks requiring spatial shifts of attention and working memory (*20–24*). Visuospatial neglect syndromes occur most frequently and are more severe after lesions in the right inferior parietal and inferior frontal cortex (*21*). Moreover, functional imaging experiments have shown that the region of superior parietal cortex identified in the present study is also engaged by successive shifts of spatial attention (*22*). Finally, differential activation of right extrastriate cortex has been reported in tasks directing attention to global aspects rather than local details of figures (*23*). But our results show that these cortical areas are also involved in a phenomenon that exhibits a number of differences compared to visuospatial attention. In contrast to shifts of attention, there is no spatial component to the perceptual transitions elicited during rivalry; moreover, whereas attentional shifts are subject to top-down influences, rivalrous transitions recur in the absence of voluntary control; finally, spatial attention also engages visual and motor areas that were not activated during rivalry (*24*). Why then should both phenomena involve overlapping regions of frontoparietal cortex? One possibility is that these areas subtend separate neural mechanisms for spatial attention and perceptual rivalry. However, it is striking that both phenomena entail the suppression of visual information from conscious perception. Monocular stimuli become periodically invisible during rivalry; similarly, sensory events associated with unattended stimuli have a diminished impact on awareness during covert attention. These effects occur in both cases in spite of a rather constant retinal input. Both phenomena may therefore call upon a common neural machinery in frontoparietal cortex, involved in the selection of neuronal events leading to visual awareness.

Thus, our results suggest that the role of frontoparietal areas in conscious perception extends well beyond that of spatial processing. Consistent with this notion, lesions of parietal and inferior frontal cortex cause disorders of nonspatial forms of perceptual selection, in addition to spatial disorders (*25*). Further investigation of frontoparietal function in both human and nonhuman primates may lead to a better understanding of the neural processes underlying the formation of perceptual states and the awareness of sensory stimuli.

REFERENCES AND NOTES

1. N. K. Logothetis and J. D. Schall, *Science* **245**, 761 (1989); F. Crick, *Nature* **379**, 485 (1996).
2. R. W. Lansing, *Science* **146**, 1325 (1964).
3. D. A. Leopold and N. K. Logothetis, *Nature* **379**, 549 (1996); D. L. Sheinberg and N. K. Logothetis, *Proc. Natl. Acad. Sci. U.S.A.* **94**, 3408 (1997).
4. The notion that rivalry involves central rather than peripheral processes goes back, at least, to Helmholtz [*Treatise on Physiological Optics* (Optical Society of America, New York, 1911)]. This view contrasts with later proposals that rivalry results from competition between monocular channels at an early stage of visual processing. For a general review of the psychophysical evidence motivating these alternative accounts, see P. Walker [*Psychol. Bull.* **85**, 376 (1978)] and R. Blake [*Psychol. Rev.* **96**, 145 (1989)]. Recent studies have shown that rivalry occurs normally when conflicting images are rapidly exchanged between the eyes, thus arguing against monocular theories [N. K. Logothetis, D. A. Leopold, D. L. Sheinberg, *Nature* **380**, 621 (1996)].
5. A. Borsellino, A. De Marco, A. Allazetta, S. Rinesi, B. Bartolini, *Kybernetik* **10**, 139 (1972).
6. J. M. Wolfe, *Nature* **380**, 587 (1996); T. J. Andrews and D. Purves, *Proc. Natl. Acad. Sci. U.S.A.* **94**, 9905 (1997).
7. Participants wore nonmetallic stereoscopic glasses and viewed a small projection screen through a mirror mounted on top of the RF coil above the participant's head. Head movements were restrained by foam pads. Stimuli were projected onto the screen by means of an LCD projector. They consisted of pairs of square images, each subtending approximately 3.5° of visual angle. Before scanning began, participants used a keypad to modify the lateral separation of the two images used during dichoptic stimulation so that each image was seen through only one eye and that stereoscopic fusion and binocular rivalry could be comfortably attained. All subsequent stimuli presented during that scanning run were then presented at those locations. Subjects indicated with two keys perceptual transitions from face to grating or vice versa, using their dominant hand. A Siemens VISION (Siemens, Erlangen) operating at 2 T was used to acquire BOLD contrast functional images. Image volumes were acquired continuously every 400 ms, each comprising 48 contiguous 3-mm-thick slices to give whole-brain coverage with an in-plane resolution of 3 mm by 3 mm. Functional imaging was performed in two scanning runs comprising 496 volumes in total. In each scanning run, after eight image volumes were discarded to allow for T1 equilibration effects, the rivalry experimental condition was presented for 41 s (10 scans) followed by the replay condition for 41 s followed by 41 s of rest. Each condition was then repeated for a total of eight repetitions per run. At the beginning of each experimental session a T1-weighted anatomical image was acquired for coregistration with the functional images.
8. Because of the slow time constants of BOLD responses (>2 s), contrasts of the face and grating stimuli were manipulated to promote long intervals between consecutive perceptual alternations, and therefore optimize the conditions for detecting neurophysiological correlates of transition events by fMRI. Frequency histograms of dominance time for the face and grating were constructed for each participant from the rivalry reports collected during the scanning session. Of the 10 volunteers that were scanned, 6 had long mean dominance times and were retained for analysis of brain activity (4 males and 2 females; mean age, 31 years; age range, 27 to 34 years; 5 right-handed and 1 left-handed; mean face dominance, 2.9 s; mean grating dominance, 5.7 s).
9. Linear regression analysis demonstrated that the temporal sequence of key-press reports during replay closely matched that of rivalry (regression slope = 1.02; $R^2 = 1$).
10. Analysis was carried out using Statistical Parametric Mapping software (SPM96, http//:www.fil.ion.ucl.ac.uk/spm). The imaging time series was realigned, spatially normalized to the stereotactic space of Talairach and Tournoux, and smoothed with a Gaussian kernel of 8 mm full width half maximum [J. Talairach and P. Tournoux, *Co-Planar Stereotaxic Atlas of the Human Brain* (Thieme, New York, 1988); K. J. Friston *et al.*, *Hum. Brain Mapping* **3**, 165 (1995); K. J. Friston *et al.*, *ibid.* **2**, 189 (1995); K. J. Friston *et al.*, *NeuroImage* **2**, 157 (1995); K. J. Friston *et al.*, *Magn. Reson. Med.* **35**, 346 (1996)]. Voxels that were activated during the rivalry and replay conditions were identified by means of a statistical model containing two components that represented the transient responses produced by the transition events in each condition, together with two boxcar wave forms that modeled and removed the condition-specific differences in mean evoked activity. The event-related changes in evoked activity were modeled by convolving an empirically derived hemodynamic impulse response function with trains of unitary events that were aligned on the reported perceptual transitions [O. Josephs *et al.*, *Hum. Brain Mapping* **5**, 243 (1997); B. R. Rosen *et al.*, *Proc. Natl. Acad. Sci. U.S.A.* **95**, 773 (1998)]. In addition, low-frequency sine and cosine waves modeled and removed subject-specific low-frequency drifts in signal [A. P. Holmes *et al.*, *NeuroImage* **5**, S480 (1997)] and global changes in activity were removed by proportional scaling. Each component of the model served as a regressor in a multiple regression analysis. The event-related components, which constitute the effects of interest, were tested to see whether they could account for a significant portion of the variance, independent of the variance attributable to the other regressors. All statistical results are based on a single-voxel Z threshold of 3.09 (corresponding to $P < 0.001$, uncorrected for multiple comparisons). Resultant regions of activation were characterized in terms of their peak heights. In assessing statistical significance, we made a correction (based on the theory of random Gaussian fields) for multiple comparisons across the whole-brain volume examined and report only regions of activation above a threshold corresponding to $P < 0.05$, corrected [K. J. Friston *et al.*, *Hum. Brain Mapping* **1**, 210 (1994)].
11. High Z scores in the group analysis reflect a significant activation averaged across individuals. The consistency of this activation was confirmed by examination of statistical contrasts for individual subjects.
12. The reconstructed postevent histograms represent an estimate of the evoked hemodynamic activity in a given voxel attributable to an individual transition event, after the effects of no interest have been removed. Each scan in each subject contributed as many sample points to this estimate as there were events in the 16 seconds preceding the acquisition of the scan. Each sample point was displaced along the time axis by the latency between the acquisition of the scan and the occurrence of the preceding event; its ordinate was calculated by adding to the value of the fitted hemodynamic response function at this latency the residual variance after complete model fitting. The sample points were used to construct a postevent histogram, with bins of 1.25 s.
13. D. C. Van Essen and J. L. Gallant, *Neuron* **13**, 1 (1994); L. G. Ungerleider and J. V. Haxby, *Curr. Opin. Neurobiol.* **4**, 157 (1994); R. Malach *et al.*, *Proc. Natl. Acad. Sci. U.S.A.* **92**, 8135 (1995); N. K. Logothetis and D. L. Sheinberg, *Annu. Rev. Neurosci.* **19**, 557 (1996).
14. N. Kanwisher, J. McDermott, M. M. Chun, *J. Neurosci.* **17**, 4302 (1997).
15. To analyze further the hemodynamic activity associated with perceptual changes in the absence of stimulus change, we tested for the presence of activity that correlated with the perceptual dominance or suppression of the face stimulus during rivalry. Compared to our main analysis of perceptual transitions per se, we expected that such a test would emphasize areas involved in the visual representation of faces, while de-emphasizing additional areas associated with transition events that are not face-specific. Areas that were significantly more active when the face was perceived than when it was not seen ($P < 0.05$ corrected) were largely confined to the fusiform gyri; maximally activated foci were located at $x = 36$, $y = -45$, $z = -24$ ($Z = 7.34$); $x = 36$, $y = -60$, $z = -21$ ($Z = 6.37$); $x = -33$, $y = -66$, $z = -15$ ($Z = 6.71$); $x = -36$, $y = -45$, $z = -24$ ($Z = 6.24$).
16. Although both rivalry and replay conditions yielded similar hemodynamic responses in the anterior cin-

gulate and SMA regions, activation in these regions was less significant during replay because of greater intersubject variability. Foci of maximal activation during replay included $x = -6, y = 9, z = 45$ ($Z = 4.69$; $P = 0.06$ corrected) and $x = 6, y = 18, z = 48$ ($Z = 4.56$; $P = 0.1$ corrected).
17. G. F. Poggio, F. Gonzalez, F. Krause, *J. Neurosci.* **8**, 4531 (1988); F. Sengpiel and C. Blakemore, *Nature* **368**, 847 (1994).
18. Superior parietal activity has not been observed during the performance of difficult visual tasks that do not involve spatial shifts of attention [M. Corbetta, F. M. Miezin, S. Dobmeyer, G. L. Shulman, S. E. Petersen, *J. Neurosci.* **8**, 2383 (1991); H. J. Heinze *et al.*, *Nature* **372**, 543 (1995); M. Corbetta, G. L. Shulman, F. M. Miezin, S. E. Petersen, *Science* **270**, 802 (1995); G. Rees, C. D. Frith, N. Lavie, *ibid.* **278**, 1616 (1997).
19. For reviews on modulation of activity by attention in ventral visual pathways, see R. Desimone and J. Duncan, *Annu. Rev. Neurosci.* **18**, 193 (1995); J. H. R. Maunsell, *Science* **270**, 764 (1995).
20. S. M. Courtney, L. G. Ungerleider, K. Keil, J. M. Haxby, *Nature* **386**, 608 (1997); S. P. O. Scalaidhe, F. A. W. Wilson, P. S. Goldman-Rakic, *Science* **278** (1997).
21. K. M. Heilman and T. Van Den Abell, *Neurology* **30**, 327 (1980); M.-M. Mesulam, *Annals Neurol.* **10**, 309 (1981); M. Husain and C. Kennard, *J. Neurol.* **243**, 652 (1996).
22. M. Corbetta, F. M. Miezin, G. L. Shuman, S. E. Petersen, *J. Neurosci.* **13**, 1202 (1993); A.C. Nobre *et al.*, *Brain* **120**, 515 (1997).
23. G. R. Fink *et al.*, *Nature* **382**, 626 (1996).
24. M. Corbetta, *Proc. Natl. Acad. Sci. U.S.A.* **95**, 831 (1998).
25. G. W. Humphreys, C. Romani, A. Olson, M. J. Riddoch, J. Duncan, *Nature* **372**, 357 (1994); M. Husain, K. Shapiro, J. Martin, C. Kennard, *ibid.* **385**, 154 (1997).
26. We thank O. Josephs and C. Büchel for assistance, R. Turner for advice on fMRI, and T. Griffiths and R. Frackowiak for comments on the manuscript. This work was funded by the Wellcome Trust.

4 February 1998; accepted 15 May 1998

Proton Transfer Pathways in Bacteriorhodopsin at 2.3 Angstrom Resolution

Hartmut Luecke,* Hans-Thomas Richter, Janos K. Lanyi*

Photoisomerization of the retinal of bacteriorhodopsin initiates a cyclic reaction in which a proton is translocated across the membrane. Studies of this protein promise a better understanding of how ion pumps function. Together with a large amount of spectroscopic and mutational data, the atomic structure of bacteriorhodopsin, determined in the last decade at increasing resolutions, has suggested plausible but often contradictory mechanisms. X-ray diffraction of bacteriorhodopsin crystals grown in cubic lipid phase revealed unexpected two-fold symmetries that indicate merohedral twinning along the crystallographic *c* axis. The structure, refined to 2.3 angstroms taking this twinning into account, is different from earlier models, including that most recently reported. One of the carboxyl oxygen atoms of the proton acceptor Asp^{85} is connected to the proton donor, the retinal Schiff base, through a hydrogen-bonded water and forms a second hydrogen bond with another water. The other carboxyl oxygen atom of Asp^{85} accepts a hydrogen bond from Thr^{89}. This structure forms the active site. The nearby Arg^{82} is the center of a network of numerous hydrogen-bonded residues and an ordered water molecule. This network defines the pathway of the proton from the buried Schiff base to the extracellular surface.

Bacteriorhodopsin is a small integral membrane protein that functions as a light-driven proton pump (*1*). Its seven-helical structure has been described (*2*–*5*) at increasing resolutions, most recently at 2.5 Å. The protein crystallizes from cubic lipid phase as thin hexagonal plates containing stacked layers of two-dimensional sheets of trimers, similar to the naturally occurring two-dimensional lattice formed by bacteriorhodopsin (*5*, *6*). The time courses of absorbance changes at 570, 410, and 640 nm after flash photoexcitation (*7*) indicate that the photochemical cycle in these crystals is nearly equivalent to that of purple membrane suspensions. We measured x-ray diffraction from these crystals. They belong to space group $P6_3$ with two trimers per unit cell, offset by ½ in *c*. In addition to the expected sixfold symmetry along the *c* axis, there are, unexpectedly, additional twofold axes in the *a*/*b* plane, as shown in Fig. 1. Given the space group for these crystals, this is an indication of merohedral twinning, a phenomenon not uncommon for certain space groups. Twinned crystals require special consideration because they are a mixture of two or more single crystals. If the twinning in these crystals were ignored, nearly 50% of the scattering matter would not be accounted for.

Taking twinning properly into account yielded a refined structure different in some respects from the one that first used crystals from cubic lipid phase (*5*). Also, the statistics of the refinement as well as the electron density maps are improved. The previously reported *R* factor and R_{free} were 22.1% and 32.7%, respectively, for data with $F > 3\sigma(F)$ between 2.5 and 5.0 Å, with an unusually high average *B* factor of 54 $Å^2$ (*5*). Calculating these parameters in the same way (omitting data higher than 5 Å), but not using a σ-based cutoff, we found the following values: *R* factor, 18.0%; R_{free}, 23.6%; and average *B*, 26.7 $Å^2$. More detailed statistical information is given in Table 1.

The overall seven-helical structure is similar to those previously determined (*3*–*5*). The loop between helices B and C forms a short antiparallel β-sheet in the same orientation as in the electron diffraction structures (*3*, *4*). We observed no density for residues 1 to 5, 154 to 166 (the loop between helices E and F), and 229 to 248 (COOH-terminus). In several positions equivalent to the diacyl lipid positions observed in one of the earlier structures from electron diffraction (*3*), we also observed long sections of density with various branch points that we interpret as native dihydrophytyl lipids, carried along through solubilization and cubic lipid phase crystallization. Model building and refinement for these areas are in progress.

The densities and the refined model at locations of interest are shown in Fig. 2. The immediate environment of the retinal Schiff base is shown in Fig. 2A. OD1 of Asp^{85}, the proton acceptor from the Schiff base in the transport cycle, is hydrogen-bonded to a water molecule, labeled W401 (*8*). OD1 of Asp^{85} also accepts a hydrogen bond from another water molecule (W402) that in turn accepts a hydrogen bond from the Schiff base, a feature predicted and much discussed (*9*) but not detected before. This water molecule and Thr^{89}, which is hydrogen-bonded to OD2 of Asp^{85} (see below), should together lower the pK_a (K_a is the acid dissociation constant) of Asp^{85} and thereby stabilize the otherwise energetically unfavorable Schiff base–Asp^{85} ion pair in the unphotolyzed protein. If the two hydrogen bond donors were displaced or entered into hydrogen-bonding with other partners after photoisomerization of the retinal, the pK_a of Asp^{85} would be raised, and this would be a reason for its protonation by the Schiff base.

The extracellular region where proton release to the surface is induced by protonation of Asp^{85} (*10*) is shown in Fig. 2B. Because titration of Asp^{85} in the dark detects the dependence of its pK_a on the

H. Luecke, Department of Molecular Biology and Biochemistry and Department of Physiology and Biophysics, University of California, Irvine, CA 92697, USA.
H.-T. Richter and J. K. Lanyi, Department of Physiology and Biophysics, University of California, Irvine, CA 92697, USA.

*To whom correspondence should be addressed. E-mail: HUDEL@UCI.EDU or JLANYI@ORION.OAC.UCI.EDU